THE ASTROPHYSICAL JOURNAL, 451:739–746, 1995 October 1

OLD ISOLATED ACCRETING NEUTRON STARS: CONTRIBUTION TO THE SOFT X-RAY BACKGROUND IN THE 0.5–2 keV BAND

SILVIA ZANE,[1] ROBERTO TUROLLA,[2] LUCA ZAMPIERI,[1] MONICA COLPI,[3] AND ALDO TREVES[1]
Received 1994 December 30; accepted 1995 April 6

ABSTRACT

The issue of the observability of old isolated neutron stars (ONSs) accreting from the interstellar gas is reconsidered using the spectra presented by Zampieri et al. In particular, we focus our attention on the overall soft X-ray emission of ONSs, which may provide a substantial contribution to the X-ray background in the 0.5–2 keV band. It is found that if accretion is channeled into polar caps by a magnetic field of $\sim 10^9$ G, up to $\sim 12\%$–25% of the unresolved soft excess observed at high latitudes in the X-ray background can be explained in terms of emission from accreting isolated ONSs. However, this would imply the detection with *ROSAT* of ~ 10 sources deg^{-2} above a threshold of $\sim 10^{-14}$ ergs cm^{-2} s^{-1}. A brief reconsideration of the observability of isolated ONSs as individual X-ray sources is also presented.

Subject headings: diffuse radiation — stars: neutron — X-rays: general — X-rays: stars

1. INTRODUCTION

Old neutron stars (ONSs), i.e., neutron stars which have evolved beyond the pulsar phase, may number as many as $\sim 10^9$ in the Galaxy. Even if their number accounts for a few percent of the total Galactic star population, isolated ONSs have not been unambiguously detected so far. Although the thermal emission resulting from cooling of the hot interior is too weak for observation after a time ~ 10 Gyr, old isolated neutron stars fed by the interstellar gas may show up as very weak, soft X-ray sources, as originally suggested by Ostriker, Rees, & Silk (1970). For a speed relative to the interstellar medium (ISM) of 10 km s^{-1} and a density of 1 cm^{-3}, the accretion luminosity L of an isolated ONS is $\sim 10^{31}$ ergs s^{-1}. If ONSs emit from their entire surface (of radius R_*) as a blackbody, the effective temperature

$$T_{\rm eff} = \left(\frac{L}{4\pi R_*^2 \sigma}\right)^{1/4}$$

turns out to be ~ 30 eV. A harder spectrum would be emitted if ONSs retain, after ~ 10 Gyr, a residual magnetic field which funnels the accretion flow in the polar cap regions: for a field of 10^9 G, $T_{\rm eff}$ could be 3 times larger at the same accretion luminosity. The low bolometric luminosity and the softness of the spectrum explain the difficulty of observing an isolated accreting ONS.

The detection of ONSs was included as a possible target for the *Einstein* mission (Helfand, Chanan, & Novick 1980), but it was only a decade later that this issue came to life again when Treves & Colpi (1991, hereafter TC) reconsidered the observability of ONSs with *ROSAT*. Assuming a blackbody spectrum, using the velocity distribution proposed by Paczyński (1990) and a local density 0.07 cm^{-3} for the ISM, they found that thousands of ONS should appear in the *ROSAT* PSPC All-Sky Survey in the most favorable case of polar accretion. A complete analysis by Blaes & Madau (1993, hereafter BM) essentially confirmed the TC results.

Recent observations with the *ROSAT* Wide-Field Camera during survey phases (Pounds et al. 1993) and with the *Extreme-Ultraviolet Explorer* (*EUVE*) have provided evidence for the presence of a relatively small number (~ 23) of unidentified bright sources: this led Madau & Blaes (1994) to rule out there being as many as 10^9 isolated ONSs in the Galaxy, if accretion is spherical. Uncertainties on the statistical properties of the old neutron star population and on the physics of the accretion process make the issue of the total number of Galactic ONSs controversial nonetheless (see, e.g., Treves et al. 1995). The search for favorable sites where accretion can make a lone neutron star shine is therefore of importance. In connection with this problem, the detectability of ONSs in molecular clouds was examined by BM and by Colpi, Campana, & Treves (1993, hereafter CCT). These studies were recently corroborated by the work of Stocke et al. (1995), in which it is proposed that a still unidentified source in the *Einstein* Extended Medium Sensitivity Survey is an ONS in the Cirrus cloud. A systematic search of isolated ONSs using *ROSAT* observations is presently underway (Danner, Kulkarni, & Hasinger 1995).

The interest in the X-ray emission from isolated ONSs is not restricted to the detection of individual sources. Despite their intrinsic weakness, in fact, they could provide a contribution to the diffuse X-ray background (XRB), since their total number is very large. This point was already discussed by BM, who found, however, that the integrated flux from ONSs is much lower than that from the XRB above 0.5 keV. In a recent paper, Hasinger et al. (1993) have analyzed the X-ray emission in selected high-latitude fields and found that the number of resolved sources exceeds by $\sim 60\%$ the number of QSOs expected from a standard evolutionary scenario. This led to the suggestion that a new population of sources can contribute sizably to the soft X-ray background detected at 0.5–2 keV with *ROSAT*. Although such a population may be extra-

[1] International School for Advanced Studies, Trieste, Via Beirut 2-4, 34014 Trieste, Italy.
[2] Department of Physics, University of Padova, Via Marzolo 8, 35131 Padova, Italy.
[3] Department of Physics, University of Milano, Via Celoria 16, 20133 Milano, Italy.

galactic in origin, Maoz & Grindlay (1995, hereafter MG) showed that its properties are compatible with those of galactic objects and tentatively identified them with cataclysmic variables (CVs). Accreting ONSs could have the desired spatial distribution but were ruled out as possible candidates by MG on the basis of their too-soft emission. We stress, however, that both BM and MG restricted their discussion to the very simple case in which the spectrum is a blackbody at $T_{\rm eff}$, emitted from the entire star surface.

In light of the previous discussion, the issue of the correct determination of the spectrum of an accreting ONS seems to be compelling indeed. In a recent paper (Zampieri et al. 1995), we addressed this problem presenting a self-consistent calculation of the X-ray spectrum emitted by an unmagnetized neutron star, solving the full radiative transfer problem for a static, plane-parallel atmosphere. It was found that, at very low accretion rates corresponding to $L \lesssim 10^{31}$ ergs s^{-1}, emitted spectra show an overall hardening with respect to the blackbody at $T_{\rm eff}$, even if the atmosphere is in LTE and the scattering optical depth is lower than the absorption depth; typical hardening factors ($\langle$radiation temperature$\rangle/T_{\rm eff}$) are about 2.5. At energies larger than 0.5 keV, where the blackbody emission becomes vanishingly small, the computed spectrum shows a persistent tail, and a fraction of 10%–20% of the total flux is emitted above this threshold.

In this paper we reconsider the observational impact of accreting ONSs using the calculated spectra and allowing for polar cap accretion. The paper is structured as follows: in § 2 we give an overview of the main points about the physics of the accretion process, and in § 3 the present distribution function of ONSs is calculated. Section 4 contains our analysis of the contribution of ONSs to the XRB, and in § 5 estimates of the observability of individual sources are presented. Discussion and conclusions follow.

2. ACCRETION ONTO ISOLATED NEUTRON STARS

The total luminosity L emitted in the accretion process depends on the star velocity v and the density of the surrounding gas n and can be written as (see, e.g., Novikov & Thorne 1973)

$$l = (1 - y)\dot{m} = 1.85 \times 10^{-3}(1 - y)nv^{-3}\,, \qquad (1)$$

where $n = (1 + \chi)n_{\rm H}$, $\chi = 0.36$ for standard chemical composition, $n_{\rm H}$ is the hydrogen number density, l, $\dot{m}$ are the luminosity and the accretion rate in Eddington units, and the velocity is in km s^{-1}. The factor $1 - y$, where $y = (1 - R_g/R_*)^{1/2}$ and R_g is the gravitational radius, is the relativistic efficiency. Typical values for the neutron star mass and radius are used throughout: $M = 1.4M_*$ and $R_* = 3R_g = 12.6$ km. In the previous formula, the star velocity is replaced by the local sound speed of the interstellar gas c_s when $v < c_s$. Alternatively, one could assume that $l \propto (v^2 + c_s^2)^{-3/2}$. It should be noted, however, that when $v \sim c_s$, both approaches give an approximated value, no simple expression for $\dot{m}$ being available (see again Novikov & Thorne 1973).

In order to evaluate the accretion luminosity, a value for $n_{\rm H}$ must be supplied. The spatial distribution of the interstellar medium in the galaxy is highly inhomogeneous (see, e.g., Dickey & Lockman 1990 for a detailed review on this subject). Observational data from Lyα and 21 cm absorption measures shows that the ISM distribution of both cold and warm H I is nearly constant in radius, while its z-dependence can be fitted by

$$n_{\rm H\,I} = n_1 \exp\left(-\frac{z^2}{2\sigma_1^2}\right) + n_2 \exp\left(-\frac{z^2}{2\sigma_2^2}\right) + n_3 \exp\left(-\frac{z}{h}\right), \qquad (2)$$

with $n_1 = 0.395$, $n_2 = 0.107$, $n_3 = 0.064$; $\sigma_1 = 212$, $\sigma_2 = 530$, and $h = 403$ pc; n_i and σ_i are in cm^{-3} and pc, respectively. The applicability of the previous expression is restricted to the range $0.4 \le R/R_0 \le 1$, where R is the Galactocentric radius and $R_0 = 8.5$ kpc is the distance of the Sun from the Galactic center. The gas layer has a scale height of about 230 pc in the vicinity of the Sun, while for $R \le 0.4R_0$ it shrinks to $\approx$100 pc and in the outer Galaxy it expands linearly up to $\approx$2 kpc. The other important contribution to the total ISM density comes from molecular hydrogen. The best tracer of H_2 is the CO molecule, and observational data suggest a local Gaussian distribution with a scale height of $\sim$60–75 pc. Observations, however, are much less conclusive as far as the midplane density is concerned (Bloemen 1987), also because it may significantly depend on R (De Boer 1991). Here we approximate the H_2 distribution with a Gaussian with central density 0.6 cm^{-3} and an FWHM of 70 pc (De Boer 1991). The ionized component gives only a very small contribution to the total density, and it will be neglected.

The remaining free parameter in our discussion is the value of c_s. If the star is moving supersonically through the ISM, the main contribution to the accretion rate comes from the material swept by its motion. On the other hand, we are mainly interested in the low-velocity tail of the distribution of the ONSs because these are the stars which radiate the higher luminosities. Their velocity may become lower than the ISM sound speed, and the accretion rate is then fixed by the thermal velocity. Since the accretion radius turns out to be always smaller than the Strömgren radius by a factor 10^3, c_s is the sound speed in a fully ionized medium at the equilibrium ionization temperature ($T \sim 10^4$ K):

$$c_s \sim 10\sqrt{(T/10^4\ {\rm K})}\ {\rm km\ s^{-1}} \sim 10\ {\rm km\ s^{-1}}\,. \qquad (3)$$

Once $n_{\rm H}$ and c_s are fixed, the observability of an ONS depends on its distance and velocity and on the response of the detector. The count rate N, corrected for the absorption resulting from the interstellar gas and for the detector effective area A_ν, is

$$N = \int_0^\infty \frac{F_\nu}{h\nu} \exp\left(-\sigma_\nu N_{\rm H}\right) A_\nu\, d\nu\,, \qquad (4)$$

where $F_\nu = L_\nu/4\pi d^2$, d is the distance of the source, $N_{\rm H}$ is the column density, and σ_ν is the absorption cross section (Morrison & McCammon 1983).

Spectral calculations are presented in Zampieri et al. (1995) for emission coming from the entire star surface and for $10^{-7} \le l \le 10^{-2}$. The lower limit corresponds to $L \simeq 2 \times 10^{31}$ ergs s^{-1} for $M_* = 1.4\ M_\odot$ and a pure H atmosphere. Since luminosities $\sim 10^{30}$ ergs s^{-1} are expected from ONSs with velocities $\sim$20–30 km s^{-1}, we have calculated model spectra down to $l = 4 \times 10^{-8}$; numerical problems prevented us from reaching lower luminosities. Spectra corresponding to $l = 10^{-7}$, 4×10^{-8} are shown in Figure 1. A comparison between the actual emerging flux and the blackbody flux above

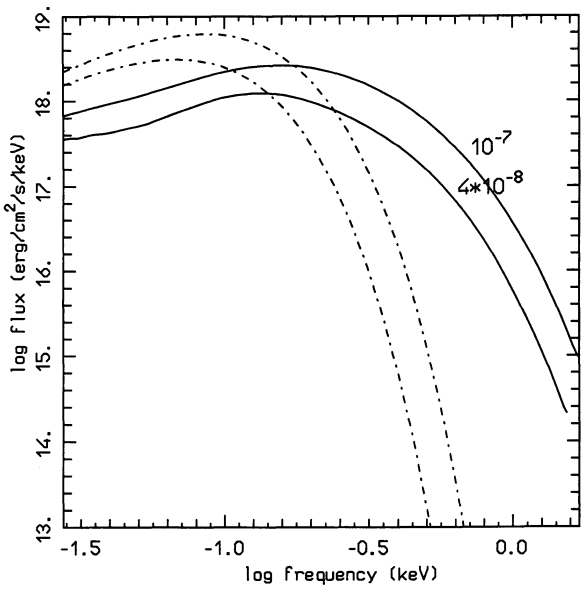

FIG. 1.—Emergent spectra for $L = 10^{-7}$ and 4×10^{-8} $L_{\rm Edd}$ (*solid lines*), together with the corresponding blackbody spectra at the neutron star effective temperature (*dashed lines*).

0.1 keV shows that the former is greater by 10%–40% and that it deviates more and more from a Planckian as luminosity decreases, showing a broad maximum. In the following sections we will be interested in evaluating the source luminosity in the 0.5–2 keV band, L_x, for any given star velocity v, or, equivalently, for any given value of the bolometric luminosity L. This is done using the analytical expression

$$\frac{l_x}{l} = 1.98 + 0.26 \log l \,, \tag{5}$$

which fits the values of l_x for numerical models to better than 4%.

We account for the presence of a relic magnetic field assuming that emission is now concentrated in the polar caps. All radiative effects of the magnetic field are neglected, so its only role is to channel the accretion flow. A different approach was considered by Nelson et al. (1995), who evaluated the contribution of the cyclotron line and supposed that the thermal part of the emission is a blackbody. For very high fields, the atmosphere is no longer in LTE, and a detailed analysis of radiative transfer including magnetic effects is required (see, e.g., Miller 1992). In addition, in this case magnetic pressure could temporarily stop the incoming flow, and the accretion process may be cyclic with recurrence time $\sim 10^6$ s (Treves, Colpi, & Lipunov 1994). For this reason, here we limit our discussion to the case of $B \sim 10^9$ G. The total emitting area is now $2A_c$, where $A_c = \pi r_c^2$ is the area of the polar cap, $r_c = R_*^{3/2} r_A^{-1/2}$, and r_A is the Alfvèn radius:

$$r_A = \left(\frac{B^2 R_*^6}{\sqrt{2GM\dot{M}}}\right)^{2/7}$$

$$= 4.3 \times 10^7 (1+\chi)^{-2/7} n_H^{-2/7} \left(\frac{B}{10^9 \text{ G}}\right)^{4/7}$$

$$\times \left(\frac{v}{\text{km s}^{-1}}\right)^{6/7} \text{cm} \,. \tag{6}$$

The limited size of the radiating region produces a hardening of the spectrum with respect to the unmagnetized case with the same luminosity, since it is now $F = L/2A_c > L/4\pi R_*^2$.

3. THE NEUTRON STAR DISTRIBUTION FUNCTION

The accretion luminosity of ONSs depends strongly on the star velocity with respect to the ISM and on the local density of the surrounding material, so in order to shed light on their collective observational properties, the knowledge of the present distribution function of ONSs in phase space is needed. Unfortunately, the velocity distribution of pulsars at birth is still poorly known, and any evolutionary scenario remains affected by this indetermination. In a detailed study, Narayan & Ostriker (1990) found that observational data of periods and magnetic fields for a sample of about 300 pulsars are well fitted by invoking the presence of two populations of neutron stars at birth, slow (S) and fast (F) rotators. These two populations differ in their kinematical properties, and the F rotators are characterized by a mean velocity and by a scale height lower than those of the S rotators. Based on this picture, the time evolution of the distribution function in the galactic potential has been studied by several authors (Blaes & Rajagopal 1991; BM; see also Paczyński 1990). In a recent paper, based on a sample of 29 young pulsars, Lyne & Lorimer (1994) suggested the possibility that neutron stars are born with typical velocities higher than both the F and S populations of Narayan & Ostriker. Their sample, however, is not complete, and this result would prima facie imply that most pulsars evaporate from globular clusters and the Galactic plane. For this reason, we retain the velocity distribution at birth proposed by Narayan & Ostriker. In any case, results presented by BM show that the contribution of high-velocity objects is really negligible as far as the observability of ONSs is concerned.

Detailed tabulations of the distribution function are not available in the literature, so we have repeated the calculations presented by BM, evolving spatial and velocity distributions corresponding to the F population of model b of Narayan and Ostriker (1990). All neutron stars were assumed to be born at $t = 0$. The Galactic potential is the sum of three contributions, disk, spheroid, and halo, and it is taken from Blaes & Rajagopal (1991). The fraction of F objects is 55% of the total number of neutron stars, and we use $N_{\rm tot} = 10^9$. The distribution function was calculated integrating the orbits of 48,000 stars, up to $t = 10^{10}$ yr. Initial conditions at $t = 0$ were obtained assuming that the velocity distribution is Gaussian in each component, together with the vertical distribution; the radial distribution is Poissonian, and the azimuthal distribution is uniform. Orbits were accepted only if the final parameters were in the ranges $0 < R < 20$ kpc, $|z| < 2.5$ kpc, and $|v| < 200$ km s^{-1}. We have found it more convenient for later applications (see the following sections) to store the distribution function in heliocentric coordinates, $f = f(r, b, l, v)$. The intervals in heliocentric coordinates and in v were divided in 75 equally spaced bins. In order to compare the output of our simulation with the results of BM, we performed the evolution of the distribution function for 20,000 stars using Galactocentric coordinates: in the local region 7.5 kpc $\leq R \leq$ 9.5 kpc, we find $\langle z^2 \rangle^{1/2} = 739$ pc; $\langle z \rangle = 261$ and 249 pc in the northern and southern hemisphere, respectively. The mean velocity in this local region, averaged over $|z| \leq 200$ pc, turns out to be 78 km s^{-1}, and $\langle v^2 \rangle^{1/2} = 87$ km s^{-1}. All of these values are in close agreement with the results of BM.

In the next sections, we will use $f(r, b, l, v)$ to estimate the observability of ONSs as X-ray sources. However, mainly in

the case of spherical emission, a detectable X-ray flux at Earth is produced only by the small number of stars that populate the low-velocity, small-r tail of the distribution. In this case a reliable statistical sample could be obtained only from the evolution of a large number of stars ($\sim 1\%$ of the total population), requiring an unacceptably high computational time. In the alternative hypothesis in which the birthrate of neutron stars is assumed to be constant, the statistics could be improved without increasing the number of computed orbits, as proposed by BM. In this case, in fact, it is convenient to store the distribution function every 10^6 yr: the final distribution can be obtained as the superposition of different outputs and will be representative of stars born at different times with the same initial conditions. In our case, however, we need to know the dependence of f on all spatial coordinates, and the storage and handling of such a high number, $\sim 10^4$, of very large matrices, $75 \times 75 \times 75 \times 75$, become troublesome.

To circumvent this problem, we have calculated the local velocity distribution $g(v)$, averaged over the region $r \leq 2$ kpc, and a best fit $G_{\rm fit}(v)$ of its cumulative function $G(v) = \int_0^v g(v')dv'$. We found that a function of the form

$$G_{\rm fit}(v) = \frac{(v/v_0)^m}{1 + (v/v_0)^n}, \qquad (7)$$

with $v_0 = 69.0$ km s^{-1}, $n \simeq m = 3.3$, provides a good fit to $G(v)$. Figure 2 shows $G(v)$ at $t = 0$, after $t = 10^{10}$ yr and $G_{\rm fit}$. In this local region, the number density of stars turns out to be $n_0 = 3 \times 10^{-4}\,(N_{\rm tot}/10^9)$ pc^{-3}, which is about 2.5 times lower than the midplane density found by BM. This apparent discrepancy is caused by the fact that we are averaging over a sphere of radius 2 kpc, centered on the Sun. By comparison, the star density computed in BM at $z = 1$ kpc is about $1 \times 10^{-4}\,(N_{\rm tot}/10^9)$ pc^{-3}. It can be seen that the relative number of low-velocity stars is higher than the initial one, reflecting the fact that these stars do not move significantly away from the Sun during their evolution, as already noted by BM. The results of the numerical simulations are also confirmed by an alternative and faster semianalytical approach based on an approximation of the third integral of the motion for low-velocity stars (BM).

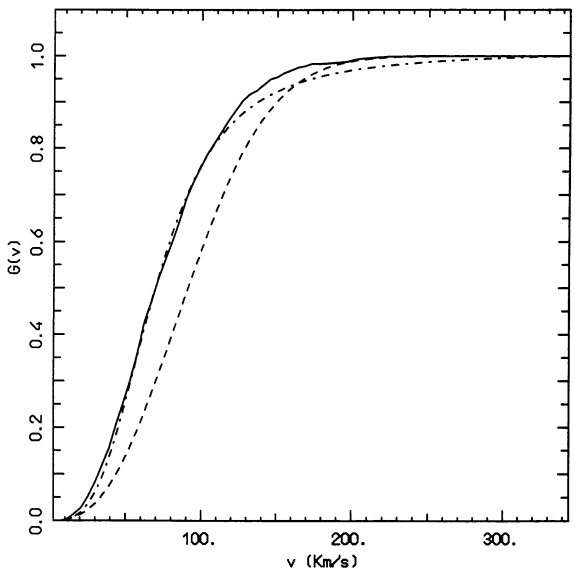

FIG. 2.—$G(v)$ at $t = 0$ (*dashed line*) and after $t = 10^{10}$ yr (*continuous line*); $G_{\rm fit}$ (*dash-dotted line*) is also shown.

4. THE CONTRIBUTION TO THE SOFT XRB

The possibility that a new, yet undetected, population of X-ray sources contributes to the X-ray background, soothing the problem of the observed soft excess, has been recently suggested by Hasinger et al. (1993). By carrying out a detailed analysis of 27 fields at high galactic latitude, $|b| \geq 30°$, these authors found that, at the faintest flux limit of *ROSAT*, about 60% of the background is resolved into extragalactic discrete sources (see also Comastri et al. 1995). Their flux is 1.48×10^{-8} ergs cm^{-2} s^{-1} sr^{-1} in the 0.5–2 keV band over a total flux $F_{\rm XRB} = 2.47 \times 10^{-8}$ ergs cm^{-2} s^{-1} sr^{-1} in the same energy band. The projected number density of resolved sources turns out to be 413 deg^{-2}, which exceeds by about 60% the density of QSOs predicted by standard evolutionary models. Even assuming that at the same flux limit the contribution of stars is $\sim 10\%$, about 120 sources deg^{-2} remain to be explained, together with $\sim 40\%$ of the XRB (soft excess). As noted by Hasinger et al., these results can be interpreted either by a more complicated model for the evolution of the X-ray luminosity function of the QSOs or by invoking the presence of a new population of sources. An important point emerging from *ROSAT* observations that sets constraints on the nature of the new population is that the average spectrum of resolved sources becomes harder at lower flux limits.

Recently MG discussed the possibility that the required new population is Galactic in origin and derived its main properties, assuming that it is composed of standard candles of fixed luminosity L. In particular, they concluded that objects with a typical X-ray luminosity $\sim 10^{30}$ ergs s^{-1}, and with a local density of $\sim 10^{-4}$ to 10^{-5} pc^{-3}, could explain a substantial fraction, 20%–40%, of the XRB, giving, at the same time, the required source density of ~ 120 deg^{-2}. Assuming a blackbody spectrum at the star effective temperature, MG have ruled out the possibility that accreting ONSs could be the proposed population, just on the basis of their spectral properties. The emitted spectrum, in fact, is too soft, with a mean photon energy ~ 30 eV for $L \sim 10^{30}$–10^{31} ergs s^{-1}. The role of the magnetic field which drastically diminishes the emitting area, and the harder spectra obtained from our calculations, together with their hardening with decreasing luminosity, lead us to reconsider the possibility that ONSs can contribute to the XRB.

Let us consider first the contribution of the entire ONS population to the XRB. Here and in the following, we use the computed distribution function and the ISM density discussed in § 2 to evaluate the actual ONS luminosity. The presence of the Local Bubble of radius ~ 100 pc surrounding the Sun has been neglected, since the fraction of stars that falls within this underdense region turns out to be negligible. The emitted flux per unit solid angle is

$$\left\langle \frac{dI}{d\Omega} \right\rangle = \frac{1}{4\pi} \int_0^{v_{\rm max}} \int_\Omega \int_0^{r_{\rm max}} f(r, b, l, v) \left(\frac{\tilde{L}_x}{4\pi r^2} \right) r^2 \, dr \, d\Omega \, dv \,, \qquad (8)$$

where the integrals in r, Ω span the entire Galaxy and $\tilde{L}_x$ is the source luminosity in the 0.5–2 keV band, corrected for interstellar absorption. The upper limit in the velocity integral is set by the fact that no synthetic spectra are available for $l < 4 \times 10^{-8}$ which corresponds to a minimum flux of 3.8×10^{17} ergs cm^{-2} s^{-1} at the source. This is of little impor-

tance, since equation (5) shows that l_x becomes vanishingly small for $l \lesssim 2 \times 10^{-8}$.

Next we consider the number of resolved sources which is given by

$$\left\langle \frac{dN}{d\Omega} \right\rangle = \frac{1}{4\pi} \int_0^{v_{max}} \int_\Omega \int_0^{d_{max}} f(r, b, l, v) r^2 \, dr \, d\Omega \, dv \, , \quad (9)$$

where d_{max} is the maximum distance at which a star of luminosity l produces a count rate above the threshold of Hasinger et al. (estimated to be $\sim 2 \times 10^{-4}$ counts s^{-1}, corresponding approximately to a flux of 2×10^{-15} ergs cm^{-2} s^{-1}). Both calculations have been repeated in the case of polar cap accretion with $B = 10^9$ G; the total column density corresponding to a given star position was used. The spatial distribution of ONSs has a characteristic scale height of ~ 260 pc, so both contributions, to the XRB and to the number count of sources, depend on direction. In order to quantify the degree of anisotropy, the two calculations have been repeated for objects with high ($|b| \geq 30°$) and low ($|b| \leq 30°$) galactic latitude. The first case allows a closer comparison with Hasinger et al. and MG.

Our results are summarized in Table 1. In the case of spherical emission, the contributions of the ONSs to the XRB is really unimportant (<1%), similar to the findings of MG and BM. Only a small fraction of stars, those in the low-velocity tail of the distribution, have spectra hard enough to give a nonnegligible contribution to the background intensity. Our result is $\sim 40\%$ greater than the estimate by BM.

In contrast, when a nonzero magnetic field is taken into account, the contribution of the ONSs to the XRB, averaged over all latitudes, is found to be of order 10%, and 5%–6% at the high latitudes considered by Hasinger et al. and MG. This corresponds to 12%–25% of the observed soft excess. As can be seen from Table 1, the contribution of the ONSs is higher by a factor 2–3 in the Galactic plane, implying a certain degree of anisotropy. However, this is not in contrast with the observed near-isotropy of the XRB at energies in the 0.5–1 keV band (see, e.g., McCammon & Sanders 1990), since ONSs can contribute at most up to 25% of the soft excess. At the sensitivity limit of the deep survey of Hasinger et al., the number density of resolved sources, averaged over all latitudes, is ~ 20 deg^{-2}, which amounts to about 5% of the total and to $\sim 18\%$ of the non-QSOs, nonstellar component.

From a direct analysis of the online catalog of the *ROSAT* PSPC pointings (ROSATSRC), we found that the mean number of sources detected with flux larger than 10^{-3} counts s^{-1} ($\sim 10^{-14}$ ergs cm^{-2} s^{-1}) is ~ 30 deg^{-2} ($b < 30°$) and ~ 40 deg^{-2} ($b > 30°$). This result is formally in agreement with the mean number of unidentified sources predicted by our model at the same flux limit, ~ 10 deg^{-2} (see the next section), although it is apparent that the ratio of ONSs over the total number of sources is unacceptably high. The contribution of ONSs to the soft X-ray background would scale as the percentage of sources which will be identified as ONSs.

The estimated contribution of the ONSs to the diffused emission is probably not strongly affected by the limits of the statistical analysis and the details of the ISM distribution, as is shown below. Assuming a mean value $n_H = 0.5$ cm^{-3}, $B = 10^9$ G and using equation (5), the X-ray luminosity is

$$l_x = \begin{cases} (3.5 \times 10^{-4} - 5.5 \times 10^{-5} \ln v)/v^3 & v \geq c_s \, , \\ 2.8 \times 10^{-7} & v \leq c_s \, . \end{cases}$$

In order to estimate the contribution provided by the most luminous stars, we can expand the approximate cumulative function, discussed in § 3, for $(v/v_0)^n \equiv x^n \ll 1$, to obtain ($m \simeq n$)

$$f(v) = \frac{dG_{fit}(v)}{dv} \simeq \frac{m}{v_0} x^{m-1}(1 - 2x^n) \, .$$

The mean source luminosity is then

$$\langle l_x \rangle \simeq \int_0^{v_{max}} l_x(v) f(v) dv \, ,$$

where v_{max} is the largest velocity at which our expansion can be reliably used. If we assume that the largest emission comes from stars within a volume V of radius 1 kpc with density $n_0 = 3 \times 10^{-4}$ pc^{-3} and at a mean distance $d \simeq 500$ pc, the contribution to the XRB turns out to be:

$$\frac{\langle l_x \rangle}{4\pi d^2} \frac{n_0}{4\pi} V = 1.23 \times 10^{-9} \text{ ergs cm}^2 \text{ s}^{-1} \text{ sr}^{-1} \sim 0.05 F_{XRB} \, ,$$

that is of the same order of that obtained from the numerical simulation.

5. OBSERVABILITY OF INDIVIDUAL SOURCES

In this section we rediscuss the observability of accreting ONSs, following previous studies on this subject (TC; BM; CCT). In particular, we refer to the PSPC on board *ROSAT*; the response curves, needed in equation (4) to obtain the count rate, are taken from the *ROSAT* guide for observers. As a result of the combined differential effects introduced by the response of the detector and the absorption of the ISM, this analysis relies crucially both on the spectral shape and on the mean photon energy.

As can be seen from equation (2), typical values for n_H are about 0.2–0.5 cm^{-3}. Higher values seem to occur in the Sco-Cen and Per directions, where $n_H \sim 1$–10 cm^{-3}. As far as the observability of individual sources is concerned, we assume

TABLE 1

CONTRIBUTION TO THE XRB OF THE OLD NEUTRON STAR POPULATION

	$\left\langle \frac{dI}{d\Omega} \right\rangle$ [a]	$\left\langle \frac{dN}{d\Omega} \right\rangle$ [b]	$\frac{\langle dI/d\Omega \rangle}{F_{XRB}} \times 10^2$	$\frac{\langle dN/d\Omega \rangle}{413} \times 10^2$
Unmagnetized.....	6.3×10^{-11}	0	2.5×10^{-3}	0
$B = 10^9$ G:				
all b.....	2.4×10^{-9}	22	9.8	5.3
$\lvert b \rvert \geq 30°$	1.3×10^{-9}	6	5.2	1.4
$\lvert b \rvert \leq 30°$	3.6×10^{-9}	38	14.5	9.2

[a] In units of ergs cm^{-2} s^{-1} sr^{-1}.
[b] In units of sources deg^{-2}.

TABLE 2

PREDICTED NUMBER OF SOURCES AND SAMPLING DISTANCES ($B = 0$)

		ALL-SKY SURVEY		DEEP-EXPOSURE	
n_H (cm^{-3})	$\bar{v}$ (km s^{-1})	d_{max} (pc)	N_{ons} ($\leq d_{max}$, $\leq \bar{v}$)	d_{max} (pc)	N_{ons} ($\leq d_{max}$, $\leq \bar{v}$)
			$L/L_{Edd} = 10^{-7}$		
0.2	9.9	525 (375)	260 (132)	1170 (725)	1293 (497)
0.5	13.	360 (240)	333 (148)	845 (425)	1837 (465)
1.	17.	275 (165)	253 (55)	675 (275)	2495 (414)
			$L/L_{Edd} = 4 \times 10^{-8}$		
0.2	14.	380 (220)	402 (135)	840 (445)	1965 (552)
0.5	19.	265 (145)	312 (51)	555 (275)	2324 (570)
1.	23.	195 (105)	262 (41)	415 (185)	2737 (544)

NOTE.—$z_{ISM} = 300$ pc.

a uniform medium and treat n_H as a free parameter. This will also allow a closer comparison of our results with those obtained in previous investigations (TC; Madau & Blaes 1994). We consider here three typical values for the density, $n_H = 0.2$, 0.5, and 1 cm^{-3}, as representative of different lines of sight.

A star of luminosity $\bar{L}$ (i.e., moving at $v = \bar{v}$) can be observed up to a maximum distance d_{max} at which the count rate N (eq. [4]) becomes lower than the sensitivity limit of the detector (1.5×10^{-2} counts s^{-1} for the All-Sky Survey, and 10^{-3} counts s^{-1} for deep exposure [DE]). Table 2 shows d_{max} for two typical luminosities, $l = 10^{-7}$ and $l = 4 \times 10^{-8}$: at distances $d \leq d_{max}$, all stars with $L \geq \bar{L}$ (i.e., $v \leq \bar{v}$) can be observed. For comparison, the corresponding quantities as derived for a blackbody spectrum are listed in parentheses.

The actual distribution function $f(r, v, l, b)$ of ONSs was derived in § 3; since the scale height of the distribution, ~ 250 pc, is comparable to that of the gas, f can also provide a reasonable estimate of the actual distribution of accreting ONSs, so we could, in principle, calculate the expected number of observable objects within d_{max}:

$$N_{ons}(\leq d_{max}, \leq \bar{v}) = \int_{\Omega} \int_0^{d_{max}} \int_0^{\bar{v}} f r^2 \, dr \, d\Omega \, dv \, , \qquad (10)$$

where r is the radial distance from the Sun. To avoid possible fluctuations resulting from the small number of slow stars in the local region present in our simulation, we replaced the previous formula with

$$N_{ons}(\leq d_{max}, \leq \bar{v}) = \begin{cases} \frac{4}{3}\pi \, d_{max}^3 \, n_0 \, G_{fit}(\bar{v}) & d_{max} < z_{ISM} \, , \\ 2\pi \, d_{max}^2 \, z_{ISM} \, n_0 \, G_{fit}(\bar{v}) & d_{max} > z_{ISM} \, , \end{cases} \qquad (11)$$

where $n_0 = 3 \times 10^{-4}$ pc^{-3}. The typical scale height for the ISM is $z_{ISM} = 300$ pc; ONSs with z larger than z_{ISM} are assumed not to accrete. The corresponding values are reported in Table 2. Equation (11) contains, nevertheless, two major simplifications: first, we assumed that locally the spatial and velocity dependence of the distribution function can be factorized; second, we considered uniformly distributed ONSs. Since this could invalidate our statistical analysis, we stress that different columns in the table do not have the same reliability. A comparison with the corresponding values calculated for a blackbody shows that maximum distances computed for actual spectral distributions are systematically higher and in high-density regions can become greater by a factor 2–3. All calculations have been repeated for polar cap accretion with $B = 10^9$ G and for the same values of l (see Table 3).

We note that stars with $l \approx 10^{-8}$ are detectable up to typical distances ≈ 200–300 pc for the All-Sky Survey, even if they emit from the entire surface. A comparison with TC results shows that these values are of the order of their estimates for polar cap accretion. However, we stress that in our case the spectral hardening is only a result of radiative processes; when a nonzero magnetic field is taken into account, objects with the

TABLE 3

PREDICTED NUMBER OF SOURCES AND SAMPLING DISTANCES (FOR POLAR CAP ACCRETION)

		ALL-SKY SURVEY		DEEP-EXPOSURE	
n_H (cm^{-3})	$\bar{v}$ (km s^{-1})	d_{max} (pc)	N_{ons} ($\leq d_{max}$, $\leq \bar{v}$)	d_{max} (pc)	N_{ons} ($\leq d_{max}$, $\leq \bar{v}$)
			$L/L_{Edd} = 10^{-7}$		
0.2	9.5	760 (705)	480 (413)	2480 (2110)	5112 (3700)
0.5	13.	685 (595)	1069 (802)	2055 (1675)	9563 (6353)
1.	16.	615 (515)	1823 (1279)	1690 (1330)	13769 (8528)
			$L/L_{Edd} = 3 \times 10^{-8}$		
0.2	15.	410 (385)	611 (539)	1350 (1060)	6630 (4088)
0.5	20.	370 (305)	1345 (914)	1160 (845)	13224 (7017)
1.	25.	340 (260)	2382 (1393)	990 (695)	20128 (9954)

NOTES.—$B = 10^9$ G; $z_{ISM} = 300$ pc.

TABLE 4

ESTIMATED OBSERVATIONAL PARAMETERS OF OLD NEUTRON STARS IN MOLECULAR CLOUDS ($B = 0$)

Cloud	d_c (pc)	R_c (pc)	n_c (cm^{-3})	CR (s^{-1})	CR_{BB}[a] (s^{-1})	v[b] (km s^{-1})	N_{ons} ($\leq v$)[b]
Cloud A	500	20	50	1.63×10^{-3}	2.05×10^{-6}	56	4
Cloud B	300	20	51	4.42×10^{-3}	5.16×10^{-6}	56	4
Cloud C	500	16	67	1.5×10^{-3}	1.46×10^{-6}	62	2
Vul Rft	400	23	61	1.67×10^{-3}	7.96×10^{-7}	60	5
Cyg Rft	700	67	29	3.3×10^{-4}	8.16×10^{-8}	47	95
Cyg OB7	800	64	29	2.73×10^{-4}	7.44×10^{-8}	47	83
Cepheus	450	45	20	2.25×10^{-3}	4.44×10^{-6}	41	18
Taurus	140	13	134	9.87×10^{-3}	3.06×10^{-6}	78	1
Mon OB1	800	34	40	4.35×10^{-4}	2.22×10^{-7}	52	15
Orion A	500	27	84	4.96×10^{-4}	8.5×10^{-8}	67	12
Orion B	500	31	56	7.78×10^{-4}	2.43×10^{-7}	58	13
Mon R2	830	32	36	$5. \times 10^{-4}$	3.87×10^{-7}	50	10
Vela Sheet	425	26	46	1.82×10^{-3}	1.27×10^{-6}	55	7
Cham	215	13	44	1.54×10^{-2}	2.4×10^{-4}	54	1
Coalsack	175	8.5	65	2.4×10^{-2}	4.32×10^{-4}	61	0
G317-4	170	5	203	1.38×10^{-2}	1.65×10^{-5}	90	0
Lupus	170	18	53	1.48×10^{-2}	2.26×10^{-5}	57	3
Rcr A	150	7.6	68	3.49×10^{-2}	8.13×10^{-4}	62	0

[a] $T_{eff} = 3.04 \times 10^{-2}$ keV.
[b] $l = 10^{-7}$.

same luminosity become visible at larger distances. As is apparent from Table 3, if the magnetic field is 10^9 G about 10 sources deg^{-2} are expected to be above the DE *ROSAT* threshold; this figure is a factor ~ 10 greater than the estimates of TC and CCT.

It has been already stressed (BM; CCT) that giant molecular clouds in our Galaxy provide the most favorable environment for the occurrence of high accretion rates. We reconsider this possibility, referring to the sample of 18 nearby clouds studied by Dame et al. (1987). Assuming that the clouds are spherical and homogeneous, the values of their radius R_c and density n_c has been calculated by CCT. A luminosity $l = 10^{-7}$, which corresponds to typical velocities in the range 40–90 km s^{-1}, has been assumed. Since velocities are largely supersonic, the use of equation (1) is fully justified. Given that the local density is much higher than the typical ISM density, we assume that all absorption is caused by the cloud material. Table 4 shows the count rate (CR) for the calculated spectrum and the expected number of observable ONSs:

$$N_{ons}(\leq v) = \tfrac{4}{3}\pi R_c^3 n_0 G(v) \; ; \qquad (12)$$

the blackbody count rate is also reported for comparison. The count rate turns out to be above the threshold of ROSAT (in DE) for more than half the clouds in the spherical case, as a result of the hardening of the spectra with respect to that of a blackbody. Clouds 15–16 and 18 appear promising also because of their high expected count rates, although the expected number of ONSs is small. We note, however, that since the number of neutron stars in the clouds is small, large statistical fluctuations are possible. The corresponding values

TABLE 5

ESTIMATED OBSERVATIONAL PARAMETERS OF OLD NEUTRON STARS IN MOLECULAR CLOUDS (FOR POLAR CAP ACCRETION)

Cloud	d_c (pc)	R_c (pc)	n_c (cm^{-3})	CR (s^{-1})	CR_{BB}[a] (s^{-1})	v[b] (km s^{-1})	N_{ons} ($\leq v$)[b]
Cloud A	500	20	50	2.05×10^{-2}	1.24×10^{-2}	54	3
Cloud B	300	20	51	5.64×10^{-2}	3.39×10^{-2}	54	3
Cloud C	500	16	67	1.97×10^{-2}	1.17×10^{-2}	59	2
Vul Rft	400	23	61	2.62×10^{-2}	1.44×10^{-2}	58	5
Cyg Rft	700	67	29	6.70×10^{-3}	3.32×10^{-3}	45	78
Cyg OB7	800	64	29	5.32×10^{-3}	2.68×10^{-3}	45	68
Cepheus	450	45	20	2.67×10^{-2}	1.66×10^{-2}	40	18
Taurus	140	13	134	0.18	9.41×10^{-2}	75	1
Mon OB1	800	34	40	6.68×10^{-3}	3.72×10^{-3}	50	12
Orion A	500	27	84	1.15×10^{-2}	5.35×10^{-3}	64	10
Orion B	500	31	56	1.44×10^{-2}	7.41×10^{-3}	56	13
Mon R2	830	32	36	6.88×10^{-3}	4.02×10^{-3}	48	10
Vela Sheet	425	26	46	2.57×10^{-2}	1.48×10^{-2}	52	7
Cham	215	13	44	0.14	9.6×10^{-2}	52	1
Coalsack	175	8.5	65	0.22	0.15	59	0
G317-4	170	5	203	0.18	0.11	86	0
Lupus	170	18	53	0.18	0.11	55	2
Rcr A	150	7.6	68	0.3	0.21	60	0

[a] $T_{eff} = 1.6 \times 10^{-2}$ keV.
[b] $B = 10^9$ G; $l_{polar\,cap} = 10^{-7}$.

for polar cap accretion are summarized in Table 5. Clouds 5–7, and 9–13 represent the most favorable sites for observability, and this agrees with the previous estimate presented by CCT.

6. DISCUSSIONS AND CONCLUSIONS

By computing the present distribution function of ONSs and using a map of neutral and molecular gas in the local region, we performed an analysis of the contribution of the ONSs to the diffuse emission in the soft X-ray energy band. A recent calculation of the spectrum emitted by accreting neutron stars (Zampieri et al. 1995) shows that, for luminosities $\sim 10^{30}$–10^{31} ergs s^{-1}, a relevant fraction (10%–20%) of the total flux is emitted in the 0.5–2 keV band even in the absence of magnetic field. Furthermore, the spatial density of ONSs in the solar neighborhood computed using the evolved distribution function turns out to be $n_0 = 3 \times 10^{-4} (N_{tot}/10^9)$ pc^{-3}. Both these values are in agreement with the constraints set by MG on possible Galactic candidates which may contribute substantially to the XRB. We found that, in the case of polar cap accretion ($B \sim 10^9$ G), when a greater number of objects produce spectra hard enough to be detectable, the contribution of the ONSs is $\approx 10\%$ of the total measured intensity in the 0.5–2 keV band, corresponding to 25%–50% of the observed soft excess. The fraction of resolved sources at the limit of the deepest ROSAT surveys is about 5%. However, the strongest constraint follows from the expected number of sources above 10^{-3} counts s^{-1}, and this will determine the importance of the contribution of the ONSs to the X-ray background.

We note that these results are not strongly dependent on the overall shape of the velocity distributions of ONSs, but only on the number of objects in the low-velocity tail, calculated here using the Narayan & Ostriker distribution function. For a high-velocity distribution at birth, such as that recently presented by Lyne & Lorimer (1994), the extrapolation to low velocities seems to indicate that the number of stars with velocity less than ~ 30 km s^{-1} turns out of the same order. However, one should keep in mind that the distribution in the low-velocity tail of ONSs remain very uncertain; for instance, it can be affected by dynamical heating, as suggested by Madau & Blaes (1994). This process, observed in the local disk star population, causes the velocity dispersion to increase with age as a consequence of scattering by molecular clouds and spiral arms (Wielen 1977). If ONSs participate in the same process, dynamical heating over the lifetime of the Galaxy may scatter a fraction of low-velocity stars to higher speeds. This could have a major effect on the source number counts (that can be decreased up to a factor of 10) and it may reduce the contribution of luminous ONSs to the background. Other factors of indetermination, like the poor knowledge about the birth rate of neutron stars, and hence, of their present total number, may affect our conclusions to the same extent. In addition, present estimates of the magnetic field of ONSs are subject to various uncertainties.

We conclude that even if neutron stars do not account completely for the characteristics of the galactic population proposed by Hasinger et al. (1993) and MG, their contribution may be of importance.

We thank the referee, Piero Madau, for some useful and constructive comments on the manuscript, Michiel van der Klis for stimulating discussions, and Tomaso Belloni for his help in extracting data from ROSATSRC.

REFERENCES

Blaes, O., & Madau, P. 1993, ApJ, 403, 690 (BM)
Blaes, O., & Rajagopal, M. 1991, ApJ, 381, 210
Bloemen, J. B. G. M. 1987, ApJ, 322, 694
Colpi, M., Campana, S., & Treves, A. 1993, A&A, 278, 161 (CCT)
Comastri, A., Setti, G., Zamorani, G., & Hasinger, G. 1995, A&A, in press
Dame, T. M., et al. 1987, ApJ, 322, 706
Danner, R., Kulkarni, S. R., & Hasinger, G. 1995, in Proc. of the 17th Texas Symposium, in press
De Boer, H. 1991, in IAU Symp. 144, The Interstellar Disk-Halo Connection in Galaxies, ed. H. Bloemen (Dordrecht: Kluwer), 333
Dickey, J. M., & Lockman, F. J. 1990, ARA&A, 28, 215
Hasinger, G., et al. 1993, A&A, 275, 1
Helfand, D. J., Chanan, G. A., & Novick, R. 1980, Nature, 283, 337
Lyne, A. G., & Lorimer, D. R. 1994, Nature, 369, 127
Madau, P., & Blaes, O. 1994, ApJ, 423, 748
Maoz, E., & Grindlay, J. E. 1995, ApJ, 444, 183 (MG)
McCammon, D., & Sanders, W. T. 1990, ARA&A, 28, 657
Miller, M. C. 1992, MNRAS, 255, 129
Morrison, R., & McCammon, D. 1983, ApJ, 270, 119
Narayan, R., & Ostriker, J. P. 1990, ApJ, 270, 119
Nelson, R. W., Wang, J. C. L., Salpeter, E. E., & Wasserman, I. 1995, ApJ, 438, L99
Novikov, I. D., & Thorne, K. S. 1973, in Black Holes, ed. C. DeWitt & B. S. DeWitt (New York: Gordon & Breach), 343
Ostriker, J. P., Rees, M. J., & Silk, J. 1970, Astrophys. Lett., 6, 179
Paczyński, B. 1990, ApJ, 348, 485
Pounds, K. A., et al. 1993, MNRAS, 260, 77
Stocke, J. T., et al. 1995, AJ, in press
Treves, A., & Colpi, M. 1991, A&A, 241, 107 (TC)
Treves, A., Colpi, M., & Lipunov, V. M. 1993, A&A, 269, 319
Treves, A., Colpi, M., Turolla, R., Zampieri, L., & Zane, S. 1995, in Proc. 7th Grossmann Meeting, in press
Wielen, R. 1977, A&A, 60, 263
Zampieri, L., Turolla, R., Zane, S., & Treves, A. 1995, ApJ, 439, 849